



Seismic Base Isolation Technologies for KALIMER

Bong Yoo, Jae-Han Lee, Gyeong-Hoi Koo, Hyeong-Yeon Lee and Jong-Bum Kim

Korea Atomic Energy Research Institute, Korea

ABSTRACT

This paper describes the status and prospects of the seismic base isolation technologies for the Korea Advanced Liquid Metal Reactor (KALIMER). The research and development program on the seismic base isolation was begun in 1993 by KAERI under the national long-term R&D program. The objective of this program is to enhance the seismic safety, to accomplish the economic design, and to standardize the plant design through the establishment of technologies on seismic base isolation for liquid metal reactors. In this paper, tests and analyses performed in the program are presented.

1. INTRODUCTION

Recently, many countries have been trying to apply seismic base isolation technology to their nuclear power plants, especially liquid metal reactors such as EFR in Europe, DFBR in Japan and PRISM in USA[1-3]. Seismic base isolation can give a significant reduction in seismic response and provide an economic benefit[4]. For seismic base isolation, it is essential to develop the isolation devices, which are to be installed between the superstructure and the basemat. For the seismic isolation device, the laminated rubber bearing (LRB) is adapted, which can support the heavy weight of the superstructure and dissipate the horizontal seismic input energy.

The contents of the R&D program are listed in Tables 1 and 2. The characteristic tests were performed for the rubber specimen, the high damping LRB(Fig.1), the lead inserted LRB[5], and the 3D-LRB. To investigate the seismic isolation capability and produce the test data for verification of the seismic analysis methodology, shaking table tests are carried out with the test model, simulating the KALIMER building and structures. The numerical methodology was developed to simulate the LRB behavior and the seismic responses of the KALIMER building and reactor structures[6-9]. Seismic analyses are performed to obtain the seismic isolation performance and the seismic margins of reactor structures.

2. TESTS FOR SEISMIC ISOLATION

2.1 Rubber Specimen Tests

The test results of rubber specimens can be obtained quickly and economically when compared to the tests of full- and reduced- scale LRBs. The type of rubber specimen tested at ANL is the 3 bar lap shear specimen, which is an LTV type as shown in Fig.2. The shear

modulus and the effective damping are calculated. The shear strain level tests for six cycles of fully reversed loading at 0.5 Hz are applied to the three specimens at the strain levels of 5, 10, 20, 50, 100, 150, 200, 250, and 300% respectively. The effective stiffness and the equivalent damping for the sixth cycle of the three specimens are represented in Fig. 3. As the shear strain increases, the shear stiffness is continuously decreased to near 150% and then increased by rubber hardening; the damping is continuously decreased as the shear strain increases.

After several hours following the shear strain tests, loading rate tests are performed on each specimen to find its sensitivity to the loading rates of 0.005, 0.05, 0.5, 1.0, and 5.0Hz, respectively, at which the six cycles at a 100% shear strain level are applied to the three specimens. Fig. 4 shows the variations of shear stiffness and damping between 0.005 Hz and 0.5 Hz.

2.2 Laminated Rubber Bearing Tests

The three types of LRB developed in the program are HLRB (High Damping Laminated Rubber Bearing), LLRB (Lead Laminated Rubber Bearing) and 3D-LRB. Two kinds of scaled HLRB and LLRB, which are to 1/4 and 1/8 scale, as shown in Fig.1, are designed, fabricated and tested, and 3D-LRB is to 1/8 scale. The 1/8-scaled LRB contains 29 rubber layers of 1.2mm thickness and 28 steel shims of 1.6mm thickness. The diameter is 150 mm. The end plate has a thickness of 25 mm and a diameter of 150mm. The total height of the LRB is 129.6 mm, and the total rubber thickness is 34.8 mm.

All tests for the reduced scale LRB are carried out at KAIST[5] and EERC (Earthquake Engineering Research Center of the University of California at Berkeley)[10]. The specific characteristic behaviors of HLRB are investigated as below.

2.2.1 Shear Strain Level Tests

The characteristic hysteretic behavior of the 1/8-scaled LRB is shown in Fig. 5. The first and the third cycle loops are plotted for shear strains of 50, 100, and 150 %, the axial stress is 2.55 MPa, and the loading frequency is 0.7 Hz. These results are for the tests up to 150 % shear strain of the respective LRB. The LRB shows less than a 10% reduction in stiffness between the first and third cycles. The effective shear modulus for LRB 1/8-04 is 1.18 MPa in the first cycle and 1.07 MPa in the third cycle. The equivalent damping is 14.2 % for the third cycle.

2.2.2 Loading Rate Effects

For evaluating the effect of loading frequency, a single test signal consisting of five cycles at strain amplitudes of 10 to 150 % is first run on a bearing at a given frequency. Thus, the LRB has then been strained to 150 %. The next test is done using another signal with strain amplitudes of 10 to 150 %, but at a different frequency. These tests are then repeated at the frequencies of 0.7Hz and 2.0 Hz (1/8-scale). Constant-velocity (saw tooth) tests at velocities of 2.12 mm/s (0.083in/s) and 4.24mm/s (0.167in/s) are also run with the axial stress of 2.55 MPa. An increase in the rate of loading leads to an increase in both the effective modulus and the equivalent viscous damping, as shown in Fig. 6. For the 1/8-scale LRB, the shear modulus increases by 12 % and the equivalent damping by about 15 % from the slow test (2.12 mm/s) to the fast test (2 Hz).

2.2.3 Axial Load Effects

For investigating the effect of axial loads for the 1/8 scaled LRB, shear cycle tests are performed at each constant strain of 25, 50, 75, 100, 125, 150, 175, and 200 %. The sequence of applied axial stresses at each strain is 2.55, 0.26, 6.37, and -0.69 MPa. The loading

frequency of the test is 0.7Hz.

Fig. 7 illustrates the influence of axial stress on the third-cycle properties of 1/8-scaled LRB; however, the conclusion that can be drawn from them is related more to load history than to axial stress. The modulus is nearly constant with axial stress. In fact, while it appears that there is a reduction in modulus as the axial stress goes from 2.55 to 0.26, then to 6.37, and then to -0.69 MPa, this is due to repeated cycling at a constant strain. These results have significant implications for the interpretation of tests and the need for the careful consideration of load history in developing test programs.

2.2.4 Shear Failure Tests

The final tests performed on the 1/8-scale LRBs are shear failure tests. Three of the four LRBs are subjected to a monotonic displacement for failure at a constant shear strain rate of 10 % per second. The applied axial stress is different for each of these tests: 2.55MPa, 6.37MPa, and 0.69MPa in tension. The fourth failure test is performed at a loading rate of 200 % strain per second, and consists of one fully-reversed cycle to 50 % strain and then a monotonic displacement for failure. This test is designed to show the influence of loading rate on the bearing failure mechanism.

The results of the shear failure tests of four 1/8-scale LRBs are presented in Fig. 8. The lowest failure occurs at 91.2mm (262% strain) for the fast failure test, with a loading rate of 200 % strain/second. There is no discernible trend based on axial load: for the three slow failure tests, the ultimate strains reached are 104.4, 101.6, 100.9mm (300, 292, and 290% strain) for axial stresses of 2.55 MPa, 6.37 MPa, and 0.69 MPa in tension, respectively.

2.3 Tests of Seismically Isolated Structures

The purposes of tests are to verify the seismic isolation performance and to produce actual test data for the practical application of LRB to the KALIMER seismic isolation design.

2.3.1 Test Model and Shaking Tables System

The test model is shown in Fig. 9, which is designed to represent the dynamic characteristics of the KALIMER. This model is composed of the rectangular basemat (16.5 tons, size of 4.3m x 4.3m x 0.6m) and four columns (0.5 ton each) supporting the slab (6.0 tons). To increase the horizontal stiffness and the safety feature of the column structure, X-type crossbars are attached to the superstructure. The seismic isolators are 1/8-scaled LRB shown in Fig. 1, and four isolators are installed under the four corners of the basemat. The hysteretic characteristics of the adopted LRB are shown in Fig. 5.

The size of the shaking table system used in the test, which can control 6 degrees of freedom motions, is 4m x 4m and the shaking capacity is 30 tons.

2.3.2 Input Motions Used in Tests

The excitation frequency band of the input random waves is from 0.5 Hz to 40 Hz and the maximum table acceleration range is from 0.1g to 0.9g.

For the shaking table tests, the three types of input motions used are the 1940 El-Centro NS, the artificial time history, and the 1985 Mexico earthquakes. All input motions are reconstructed through the band limited filtering of original data from 0.07Hz to 25Hz. With consideration of the similarity of the 1/8 scaled down system, the time interval of input motions is re-scaled from 0.02 second to 7.07 ms.

2.3.3 Test Results and Discussions

Fig. 10 shows the variations of the seismic isolation frequencies corresponding to the

maximum peak input accelerations obtained from random tests. In the results, as the excitation levels increase, the seismic isolation frequencies of a seismically isolated structure decrease. This result indicates that the horizontal stiffness of LRB is evidently changed with the shear strains. The fundamental frequencies of X and Y directions are about 7 Hz and 6 Hz for the case of the seismic isolation, and 6 Hz and 5 Hz for the fixed base case respectively.

Fig. 11 shows the results of the floor response spectrum at the slab. For cases using the 1940 El-Centro NS and the artificial time history earthquakes, the seismic responses are significantly reduced. However, the 1985 Mexico earthquake, in which the dominant excitation frequency is 1.3Hz, produces severe resonant responses in structures. In reality, it is not expected that a type of earthquake similar to the 1985 Mexico earthquake containing very long period components tuning the seismic isolation frequency will occur at a hard rock nuclear power plant site. Therefore, the 1985 Mexico earthquake may be treated as a hypothetical or the worst loading case in seismic isolation design.

In the cases of the 1940 El-Centro and the artificial time history earthquakes, the maximum shear deflections of LRB in tests are both lower than 50%(17.5mm) shear strain for a 0.3g and 200%(70.0mm) for a 0.9g. When considering a SSE (Safe Shutdown Earthquake) load of 0.3g in the KALIMER seismic design, the safety margin of LRB is enough to cover the design requirements of the minimum failure shear strain of LRB, 300%[11]. For the 1985 Mexico earthquake, resonant responses occur and LRB shows large shear deflection responses.

Fig. 12 shows the test results of the maximum peak acceleration responses at the slab for various magnitudes of each input motion. For the cases of the 1940 El-Centro and the artificial time history earthquakes, the seismic responses are significantly reduced by about 8 and 6 times respectively for a 0.3g input magnitude compared with those of the non-isolated system. However, as previously mentioned for the 1985 Mexico earthquake, a counter result of the seismic isolation effects occurs in seismic responses.

3. NUMERICAL SIMULATION OF A SEISMICALLY ISOLATED KALIMER

Analysis methodologies using finite element methods are developed to predict the behaviors of LRB used for KALIMER isolation. The numerical simulations verified have been applied to the response analyses of the reactor building, reactor structures and components.

3.1 Shear Deformation Analysis for Laminated Rubber Bearings

The finite element analyses for shear deformation of the KAERI HLRB made of MRPRA rubber compounds are performed. In those, the hyperelastic material option of ABAQUS for the strain energy functions is used for modeling rubber layers. The 2D harmonic elements and 3D solid elements are used in finite element analyses, and three kinds of strain energy density functions calculated with four kinds of rubber compound test data are used in modeling the rubber layers [9].

For a 2D model, the element types for steel shims and rubber layers are the CAXA41 and CAXA8H1, respectively, which have an axisymmetric geometry with a non-axisymmetric load. For the 3D model, the 3D solid element of C3D8H is used. The boundaries are fixed at the bottom of the bearing, vertically coupled and horizontally freed at the top of the bearing. The Young's modulus and Poisson ratio of the steel shims are chosen as 200 GPa and 0.3 respectively. The horizontal displacements are applied from 0% to 300% of the total rubber height under the vertical pressure of 2.55 MPa.

In 2D model, the number of elements for a rubber layer is three in the thickness direction. According to the material models for rubber, there are some different results, as shown in

Fig.13(a). The analyses with the Mooney-Rivlin and Polynomial ($N=2$) models gives quite a discrepancy with the test results, but the analysis with the Ogden ($N=3$) method results in a relatively good agreement with the test results up to a shear displacement of 63 mm(equivalent to 180% shear strain).

In 3D solid model, one element in the thickness direction is used for a rubber layer. Force and displacement relations are represented in Fig.13(b). The results using the Ogden model are closer to the test data, as in case of the 2D model.

3.2 Seismic Analysis for Reactor Building

For obtaining the time history of the seismic responses of reactor building as shown in Fig. 14, a lumped-mass beam model is developed as shown in Fig.15. The model is composed of two sticks; the one is for the reactor building and the other is for the reactor support structure. The time history responses for the non-isolated and isolated reactor buildings are calculated for an artificial time history earthquake, which is generated by using the seismic design spectrum curve of US NRC RG1.60.

The isolation frequency of the reactor building is 0.5 Hz and the equivalent damping of LRB is 12%. The horizontal stiffness of the total isolator is 5.77×10^8 N/m and the damping coefficient is 4.356×10^7 N.sec/m. The total weight is about 68,000 tons. The first frequencies for x, y, z directions of the isolated reactor building are 10.1Hz, 8.73Hz, 12.8Hz, respectively.

For the artificial time history (ATH), the maximum acceleration responses of the non-isolated and isolated reactor buildings for the horizontal and vertical earthquake data are shown in Table 3. The displacement responses of x-direction are presented in Fig. 16. The response spectra at major locations are represented in Fig.17. For the horizontal seismic input of 0.3g ZPA, the maximum acceleration is reduced to 0.177g for an isolated condition, while one is 1.46g for a non-isolated condition. The maximum displacement is larger to 15.0cm for the isolated condition. The maximum acceleration for the vertical earthquake of 0.208g ZPA is amplified to 0.848g for the isolated condition, while the one is amplified to 0.557g for the non-isolated condition. This agrees with the general trend that the horizontal isolation of a structure can amplify the vertical responses [1-3].

3.3 Seismic Analysis for Reactor Structures and Components

For the preliminary investigation of the seismic isolation effects on KALIMER reactor internals as shown in Fig.18, the seismic analyses are carried out with a lumped-mass model. Using the 3-dimensional finite element model, detail local stiffness analyses are performed to construct the lumped-mass seismic analysis model shown in Fig.19. The hydrodynamic mass of primary sodium is implemented to the model. The seismic analysis and evaluation are presented through the modal analysis, the seismic time history analysis, and the equivalent seismic stress analysis.

Table 4 shows the natural frequencies of the reactor structures. For the non-isolated system, the dominant fundamental coupled mode of whole reactor internal structures including reactor vessel is 8.1Hz. This fundamental frequency is increased to 11.5Hz when the seismic isolation is applied to the fixed basemat system. Therefore, when considering the assumed seismic isolation frequency of 0.7Hz, the significant horizontal response reductions are expected. The first and second natural frequencies are 1.9Hz and 8.1Hz in vertical direction.

The seismic design loads used in this analyses are OBE(0.15g) and SSE(0.3g). The same seismic input motions are used in both the horizontal and vertical directions. To investigate the seismic responses for beyond the design basis(BDB), the postulated 1.0g seismic event is used. The synthetic acceleration time history contains enough number of peaks enveloping the

NRC Reg.1.60 seismic design spectrum.

The seismic responses of reactor structures of the seismically isolated KALIMER are significantly reduced for accelerations and relative displacements in the horizontal direction as shown in Tables 5 &6. For the isolation case, the maximum peak accelerations in the horizontal direction for the all structures and components is 0.11g for OBE and 0.22g for SSE. The responses are reduced about 14 times in IHX, 9 times in EMP and 8 times in the reactor vessel liner, support barrel, and core compared with those in the non-isolated case. However, for the vertical direction, significant response amplifications occur in whole structures. This is due to the vertical structural frequency of 8.1Hz located in the dominant excitation frequency band of the input motion.

Essentially, single-frequency response of the isolated system permits the reactor seismic stresses to be based on equivalent static analysis using the inertia loads obtained by applying the amplification factors calculated in system dynamic analyses. The results of the seismic analysis for seismically isolated KALIMER show that there are no seismic response amplifications in horizontal responses of the reactor structures and components.

The equivalent seismic loads are OBE of 0.11g and SSE of 0.22g for the horizontal direction and OBE of 1.97g and SSE of 2.94g, which are including the gravity effects of 1.0g, for the vertical direction. Not like the horizontal responses, the vertical responses are different in each structure but the maximum peak acceleration is selected as conservative. The horizontal and vertical loads are simultaneously applied in stress analysis.

The seismic margin evaluations are performed using the stress limit conditions of ASME Code, Section III, Appendix F, Rules for Evaluation of Service Loadings with Level D Service Limits. Table 7 shows the results of the seismic margin evaluations and the seismic capacity. From the results, the containment vessel, reactor vessel, inlet plenum, and core support have large seismic stress margins but the reactor vessel liner, support barrel, separation plate, and baffle plate have small margins. The maximum stress occurs in reactor vessel liner parts connected with the separation plate due to the vertical seismic loads.

The maximum seismic resistance in the reactor internal structures is evaluated as 0.354g by the index of seismic capability(SC) defined in Table 7.

4. CONCLUSIONS

The R&D program on seismic base isolation technologies for the KALIMER established in 1993 has made important progress in validating the isolation technologies essential to enhancing the seismic safety, and the economic structural design.

The various tests for rubber specimens, LRBs, and isolated structural model, and the numerical simulations for the evaluation of LRBs and seismically isolated KALIMER structures have been done in this program to verify the performance and the effectiveness of the seismic base isolation.

Further R&D on seismic isolation techniques will produce fruitful results to enhance the structural safety of the KALIMER subjected to design basis earthquakes as follows;

- Development of 3D isolator that can reduce both horizontal and vertical seismic responses, while the horizontal base isolation only has a benefit on the horizontal direction.
- Development of seismic isolation design guidelines for the KALIMER from the future R&D program and collaboration with foreign countries.
- Large scale structural tests for the KALIMER including reactor vessel, reactor core, piping systems, etc to verify the seismic isolation design.

Acknowledgement

This work was performed under the long term nuclear R&D program sponsored by the Ministry of Science and Technology of Korea.

References

1. Proc. of the First International Seminar, "Seismic Base Isolation for Nuclear Facilities," San Francisco, Cal., USA, A Post Conf. Seminar of the 10th Int'l. Conf. on SMIRT-10, USA, 1989.
2. Proc. of 11th SMIRT Post Conf. Seminar, "Seismic Isolation of Nuclear and Non-nuclear Structures," Nara, Japan, 1991.
3. Proc. of Int'l Post-SMIRT(13th) Conf. Seminar, "Seismic isolation, passive energy dissipation and active control of vibrations of structures," Santiago, Chile, 1995.
4. Yoo, B., Lee, J.H., Koo, G.H. and Y.-H. Kim, "Effects of High Damping Rubber Bearing on Seismic Response of Superstructure in Base Isolated System," 13-th SMiRT, Brazil, 1995.
5. Yoo, B., Lee, J.H. and Koo, G.H., "Study of Reduced-Scale Model Test Results of High Damping and Lead Laminated Rubber Bearing for Liquid Metal Reactor," KAERI/TR-809/97, 1995 (in Korean).
6. Yoo, B., Lee, J.H., Koo, G.H. and Lee, D.G., "Seismic Isolation for Nuclear Reactors in Korea," Int. Post-SMiRT Conf. Seminar on Seismic Isolation, Passive Energy Dissipation and Control of Vibrations of Structures, Santiago, Chile, 1995.
7. Yoo, B et al, "Analytical Modeling and Seismic Response Analyses of KALIMER Reactor Building," KNS, Proceedings of 98 Spring Conference, 1998, pp.903-908 (in Korean)
8. Yoo, B., Koo, G.H. and Lee, J.H., "Conceptual Design by Analysis of KALIMER Seismic Isolation," KAERI/TR-697/96, 1998.
9. Yoo, B. and Lee J.H., and Koo, G.H., 3rd IAEA Research Co-ordination Meeting on "Intercomparison of Analysis Methods for Seismically Isolated Nuclear Structures," UK, 1998.
10. Kelly, J.M., Aiken, I.D. and Clack, P.W., "Experimental Testing of Reduced-Scale Seismic Isolation Bearings for Nuclear Application," Proc. of the Int. Post-SMiRT Conference Seminar, Taormina, Sicily, Italy, 1997.
11. Yoo, B., Koo, G.H. and Lee, J.H., "Development of Guidelines for Seismic Isolation Design of LMR," Proceedings of Earthquake Engineering Society of Korea, 1998, pp.147-154 (in Korean).

Table 1. Test Programs on Seismic Isolation Technology for KALIMER

Items	Years								Joint Work on Test & Fab.	Remarks
	93	94	95	96	97	98	99			
Rubber Specimens									UNISON(Fab.)	
-Shear Dynamic Test									ANL & ENEL	
-Uniaxial Tensile Test									ENEL	
-Equibiaxial Tensile Test									ENEL	
-Planar(pure shear) Test									ENEL	
-Volumetric Test									ENEL	
Rubber Bearings									UNISON(Fab.)	
-HLRB(1/4 & 1/8 scales)									GE/EERC(*)	
-LLRB(1/4 & 1/8 scales)									& KAIST	
-3DLRB(1/8 scale)									KAIST	
Isolated Model Structure									UNISON(Fab.)	
-Fixed									KIMM	30ton, 6DOF (4m x 4m)
-2D isolation(1/8scale)									KIMM	"
-3D isolation(1/8scale)									KIMM	"

Table 2. Numerical Evaluation Models for Rubber Bearings and Isolated Structures

Items	Numerical Models		Computer Code	Remarks	
LRB & LLRB	Rubber	<ul style="list-style-type: none"> Strain Energy Functions -Mooney Rivlin/ -Polynomial -Ogden/ -Seki 		ABAQUS SMiRT 13&14	
	Steel Shim	<ul style="list-style-type: none"> Linear Elastic 			
	Lead	<ul style="list-style-type: none"> Elastic-Plasticity Constitutive Law 			
LRB Structure behaviors for Isolated Structures	<ul style="list-style-type: none"> Linear Model Bilinear / Modified Bilinear Model Rate Model 		ABAQUS User Subroutine		
Reactor Core	<ul style="list-style-type: none"> Nonlinear Model 		SAC-CORE	ASME PVP '98	

Table 3. Acceleration Responses of KALIMER Building for ATH Earthquake

Location	X-Direction(g)		Y-Direction(g)		Z-Vertical (g)	
	Isolated	Non-isolated	Isolated	Non-isolated	Isolated	Non-isolated
Base	0.175	0.30	0.177	0.30	0.321	0.205
Top	0.177	1.461	0.179	1.609	0.848	0.577
RV support	0.173	0.583	0.175	0.676	0.558	0.362

Table 4. Natural Frequencies of KALIMER Reactor Structures

Mode	Horizontal (Hz)		Vertical (Hz)	
	Isolation	Non-isolation	Isolation	Non-isolation
1	0.70	8.11	1.87	1.87
2	11.51	11.88	8.09	8.25
3	13.69	18.81	17.77	17.94
4	21.04	27.85	23.08	34.26
5	27.90	27.97	34.85	36.59

Table 5. Results of Zero Period Accelerations for Isolated System

Items	Horizontal ZPA (g)			Vertical ZPA (g)		
	OBE (0.15g)	SSE (0.3g)	BDB (1.0g)	OBE (0.15g)	SSE (0.3g)	BDB (1.0g)
CV	0.11(0.17)	0.22(0.34)	0.73(1.13)	0.15(0.14)	0.30(0.28)	1.00(0.93)
RV	0.11(0.64)	0.22(1.28)	0.73(4.27)	0.17 (0.16)	0.34(0.32)	1.13(1.07)
IHX	0.11(1.56)	0.22(3.12)	0.73(10.4)	0.16(0.14)	0.32(0.28)	1.07(0.93)
EMP	0.11(0.98)	0.22(1.96)	0.73(6.53)	0.16(0.14)	0.32(0.28)	1.07(0.93)
RV Liner	0.11(0.95)	0.22(1.90)	0.73(6.33)	0.97(0.97)	1.94(1.94)	6.47(6.47)
SB	0.11(0.92)	0.22(1.84)	0.73(6.13)	0.67(0.66)	1.34(1.32)	4.47(4.40)
UIS	0.11(0.15)	0.22(0.30)	0.73(1.00)	0.16(0.14)	0.32(0.28)	1.07(0.93)
Core	0.11(0.88)	0.22(1.76)	0.73(5.87)	0.94(0.91)	1.88(1.83)	6.27(6.07)

() : for non-isolation system

Table 6. Results of Displacement Responses

Loads	Isolator Deflections (cm)		Rel-Disp. Between UIS and Core (cm)	
	Horizontal	Vertical	Horizontal	Vertical
OBE (0.15g)	5.266	0.018	0.045(0.379)*	0.485(0.456)*
SSE (0.3g)	10.531	0.035	0.089(0.758)*	0.970(0.913)*
SC (0.354g)	12.428	0.043	0.106(0.894)*	1.145(1.076)*

SC : Seismic Capacity, () * indicates the results of non-isolated system.

Table 7. Seismic Margin and Seismic Capacity of KALIMER Reactor Structures

Items	σ_{SSE} * (MPa)	P_{L+b} * (MPa)	Margins *	Min. Seismic Capacity *
Containment Vessel	21.4	401.9	17.78	
Reactor Vessel	39.6	401.9	9.15	
RV Liner	340.0	401.9	0.18	
Support Barrel	113.0	382.4	2.38	
Inlet Plenum	20.8	401.9	18.32	
Separation Plate	188.0	401.9	1.14	
Baffle Plate	193.0	382.4	0.98	
Core Supports	72.1	401.9	4.57	

* σ_{SSE} = Total stress intensity for horizontal and vertical SSE loads

* P_{L+b} = $1.5 \times \text{Min} [2.4 S_m, 0.7 S_u]$, ASME Code Sec.III App.F.

* Margin = $(P_{L+b} / \sigma_{SSE}) - 1$

* Seismic Capacity = Min[Seismic Stress Margin +1] x SSE

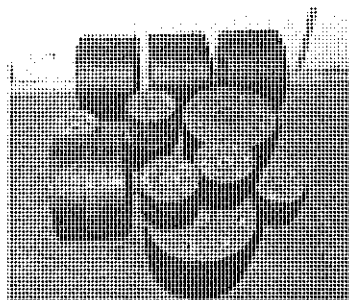


Fig. 1 Scaled Laminated Rubber Bearings

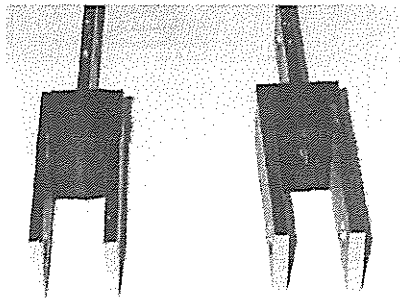


Fig. 2 Rubber Specimen for Shear Dynamic Test

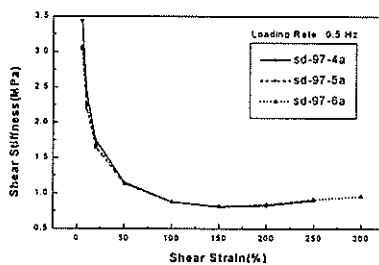


Fig. 3 Equivalent Shear Stress and Damping vs. Shear Strain for Rubber Specimen

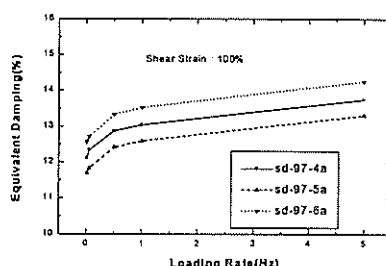
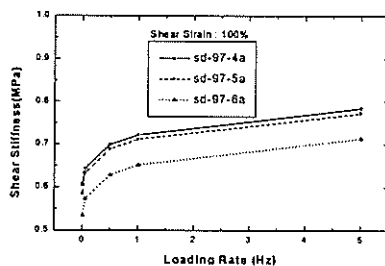
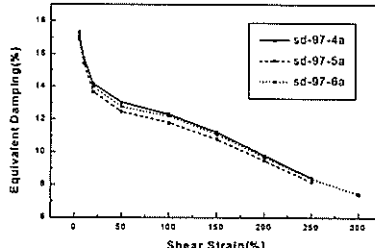


Fig. 4 Equivalent Shear Stress and Damping vs. Loading Rate for Rubber Specimen

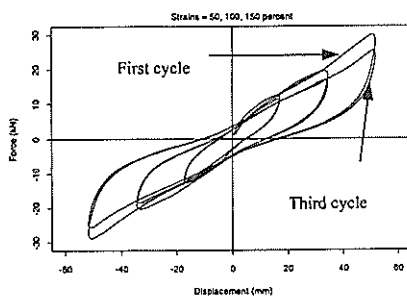


Fig. 5 Hysteretic Behavior of HLRB 1/8-04

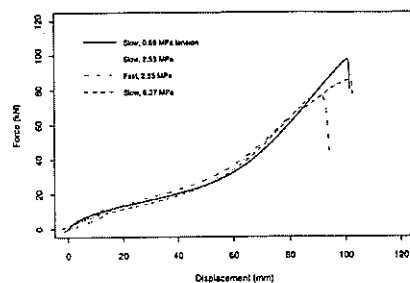


Fig. 8 Shear Failure Tests of 1/8 Scale Bearings

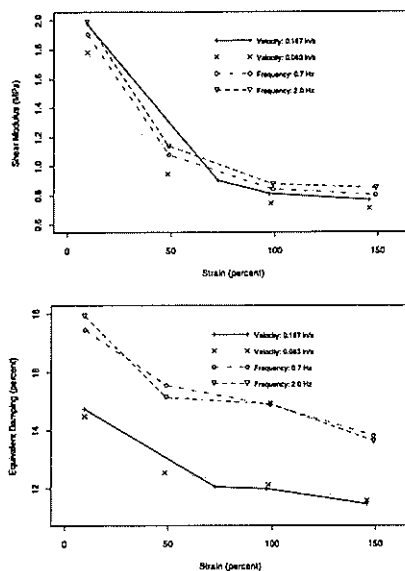


Fig. 6 Dependence on Loading Rate, HLRB 1/8-04 Fig. 7 Dependence on Axial Stress, HLRB 1/8-03

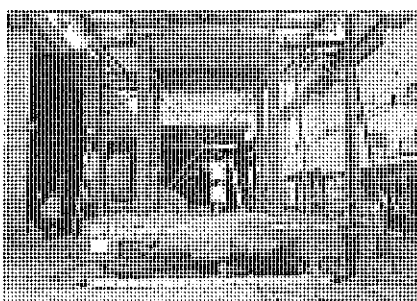
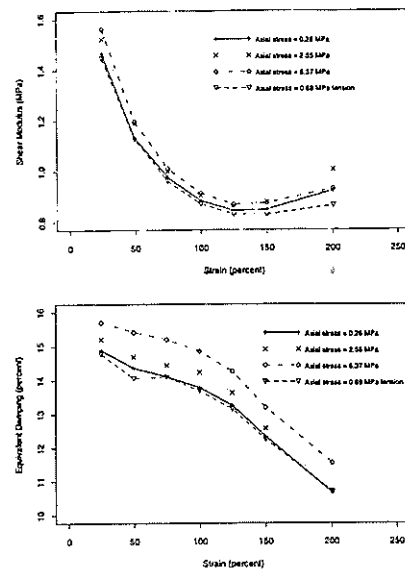


Fig. 9 Seismically Isolated Test Model

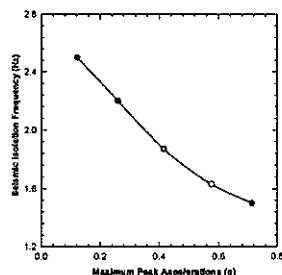


Fig. 10 Isolation Frequencies vs. Base Exciting Acc.

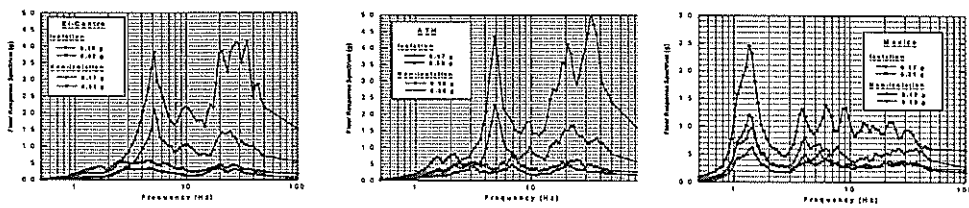
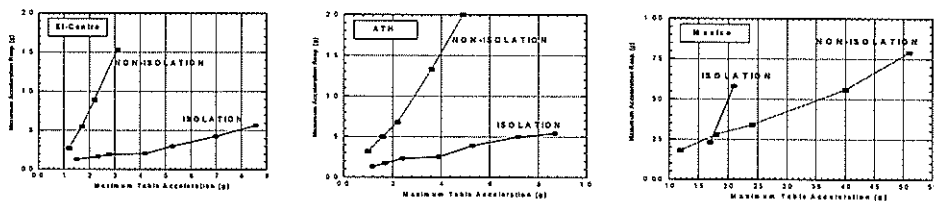


Fig. 11 Floor Response Spectrum at Slab

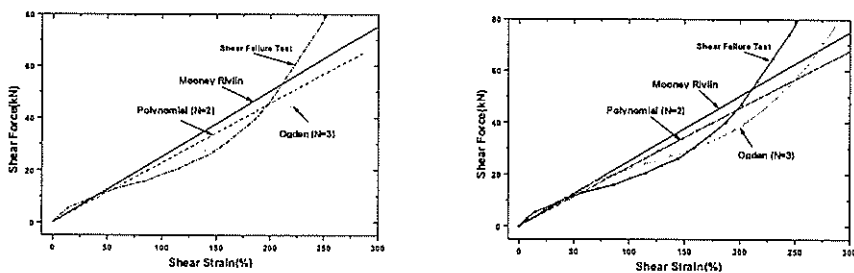


(a) 1940 El-Centro NS

(b) Artificial Time History

(c) 1985 Mexico

Fig. 12 Test Results of Seismic Isolation Frequencies



(a) 2D, No. of Elements for a Rubber Layer : 3

(b) 3D, No. of Elements for a Rubber Layer : 1

Fig. 13 Shear Forces vs. Shear Strain of Rubber Bearing

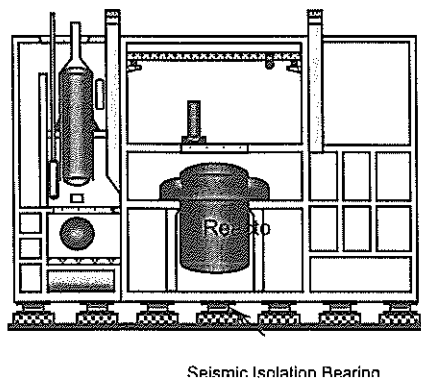


Fig. 14 KALIMER Reactor Building

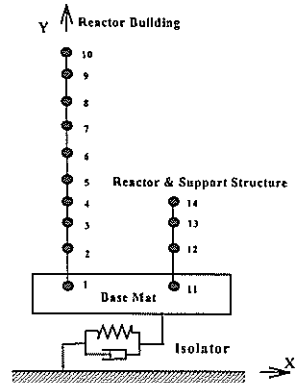


Fig. 15 Lumped Mass-Beam Models
of KALIMER Building

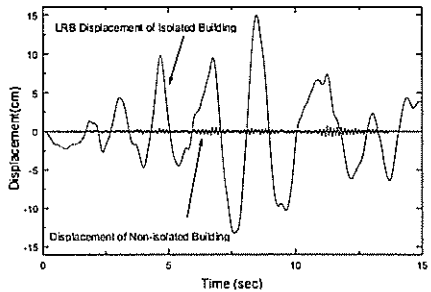


Fig. 16 Displ. Responses of Reactor Building
(Artificial Time History Input)

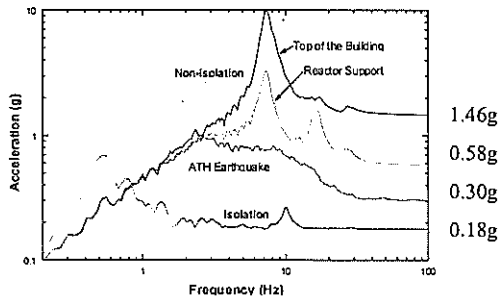


Fig. 17 Accel. Resp. Spectra of Reactor Building
(ATH, X-dir. 0.3g)

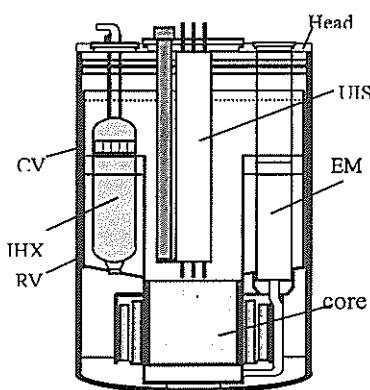


Fig. 18 KALIMER Reactor Structure
and Components

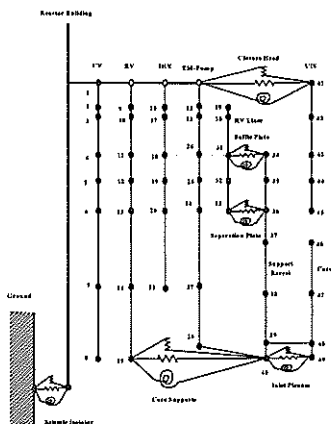


Fig. 19 Seismic Analysis Model of KALIMER
Reactor Structure and Components